Desalination and Water Treatment
www.deswater.com
doi: 10.5004/dwt.2020.25962

192 (2020) 451–457
July

Temperature dependence of TransMembraneChemiSorption for wastewater with ammonia contents

J. Lakner[a], G. Lakner[a,*], P. Bakonyi[b], K. Belafi-Bako[b]

[a]*Hidrofilt Kft, Magyar utca 191, 8800 Nagykanizsa, Hungary, Tel. +36 30 579 7930; Fax: +93 536 500; emails: lakner.g@hidrofilt.hu (G. Lakner), lakner.jozsef@amk.uni-obuda.hu (J. Lakner)*
[b]*University of Pannonia, Research Institute on Bioengineering, Membrane Technology and Energetics, Egyetem út. 10, 8200 Veszprem, Hungary, Tel. +36 30 916 6331; Fax: +88-624292; emails: bako@almos.uni-pannon.hu (P. Bakonyi), bakonyi@almos.uni-pannon.hu (K. Belafi-Bako)*

Received 18 October 2019; Accepted 8 April 2020

ABSTRACT

Ammonia is a common contaminant of household and industrial wastewater. Several procedures can remove it, with membrane contactors playing a key role here. Several models were developed for the process mechanism; the mass transfer coefficient is the most important characteristic for all of them. The value of the mass transfer coefficient depends on the characteristics of the membrane and the wastewater, the most important of which is the treatment temperature. In a previous study, the mass transfer coefficient was determined as a function of temperature. Using a single-process model and a so–called Arrhenius-type correlation for the temperature dependence of the mass transfer coefficient, the activation energy obtained was much smaller than the measured values. The results obtained by the improved multi-process model presented in this paper already correspond to those of the experiments. By comparing these values the model makes it possible to estimate the ratios of the sub-processes taking place during the mass transfer process, and through this to define which parameters determine the mass transfer coefficient and how it can be increased by changing these parameters.

Keywords: Ammonia removal; Membrane contactor; Water treatment; Temperature dependence; Diffusion; Activation energy

1. Introduction

Ammonia is a common contaminant of household and industrial wastewater. Its excessive presence in the receiving media can create a serious contamination risk. Several procedures can remove it, with membrane contactor (TransMembraneChemiSorption – TMCS) procedures being particularly significant from both a technical and economic perspective [1–8].

The mass transfer process is characterized by the (total) mass transfer coefficient, the value of which is dependent relatively strongly on temperature, and increases with it [9–11]. The mass transfer process is usually considered a diffusion process, so its temperature dependency is determined by that of the latter. The so–called Knudsen diffusion generally used to describe diffusion through a membrane [10] is virtually independent of temperature. This suggests that the (total) mass transfer coefficient is primarily determined not by intra-membrane diffusion but by some other factor.

In a previous study, the mass transfer coefficient was determined as a function of temperature [12]. In this work, using a single-process model [13], the mass transfer process was interpreted as a transition across a potential barrier, which displays the so–called Arrhenius-type temperature dependence for the mass transfer coefficient. The activation

* Corresponding author.

Presented at PERMEA 2019, 26–29 August 2019, Budapest, Hungary

energy obtained in this case is much smaller than the measured values, therefore the whole process is interpreted as two sub-processes, with liquid diffusion taking place through the feed-side boundary layer and through the membrane [14].

In this case, the temperature dependence is given by that of the Henry-constant and viscosity, expressing the ratio of (gaseous) ammonia concentration in the melt and the membrane. The temperature dependence calculated this way already confirms the values measured. Furthermore, the model also enables us to compare the proportions of the two sub-processes relative to each other.

2. Theory

2.1. Ammonia in a watery solution

Ammonia in an aqueous solution is present as free ammonia (gaseous ammonia, NH_3) and ammonium hydroxide (NH_4OH, NH_4^+). The proportions depend on temperature T and the pH of the solution [13]. Free ammonia is able to pass through the membrane, so it is important to examine this from both a theoretical and practical point of view. In the temperature range used (20°C–50°C), with pH > 11 – which can be ensured by alkalization – ammonia should be present in the solution in the form of free ammonia [11]. Below, ammonia concentration means the concentration of free ammonia [NH_3] [12].

2.2. Mass transfer coefficient

In the case of diffusion, the flux is mass, the driving force is the negative gradient of concentration, and the ratio coefficient is the D diffusion constant, that is:

$$J = -D \cdot \mathrm{grad}\left[\mathrm{NH_3}\right] \tag{1}$$

which is known as Fick's first equation. With heterogeneous media, in Eq. (1), the effective diffusion coefficient $\tilde{D}$ must be considered instead of D [14,15].

The free ammonia passes through the membrane with a transport process (mass transport). Let us assume the system consists of two (feed and receiving) boxes separated by a flat sheet membrane (Fig. 1), furthermore, the concentration distribution is homogenous in both boxes (full mixing in liquid), which can be achieved by mixing. In this case, the number of molecules passing through a cross-section unit per time unit, the (total) molar ammonia flux [16]:

$$J = K\left(\left[\mathrm{NH_3}\right]_f - \left[\mathrm{NH_3}\right]_s\right) = K\left[\mathrm{NH_3}\right]_f \tag{2}$$

will be proportional to the concentration difference between feed ($[NH_3]_f$) and (receiving) stripping side ($[NH_3]_s$) [12]. In Eq. (2) the stripping-side ammonia concentration can be considered $[NH_3]_s = 0$ [17–20] since the rate constant of the stripping process after the mass transfer process is several magnitudes greater than that of diffusion [12].

K is the (total) mass transfer coefficient (single-step model) [13,17–18], which is:

$$K = \frac{\tilde{D}}{d_m} \tag{3}$$

where d_m is the (characteristic) thickness of the membrane (Fig. 1).

2.3. Temperature dependence of the mass transfer coefficient

The mass transfer coefficient strongly depends on temperature [12]. Transport and chemical processes are thermally activated processes, so the rate constant of the mass transfer process through the membrane – as for all processes of this type – exhibits an Arrhenius-type temperature dependence [21], namely:

$$K = K_0 e^{-\frac{E_a}{R_g T}} \tag{4}$$

where K_0 is the pre-exponential coefficient that can be marginally dependent on temperature, E_a is the activation energy of the process, and R_g is the gas constant. As can be seen on Eq. (4), if the temperature rises, the mass transfer coefficient also increases.

2.4. Membrane contactor

The membrane contactor (TMCS) is a recirculation system, where wastewater to be treated circulates on the feed side, and – usually in the opposite direction – solvent liquid on the receiving side; in the case of ammonia removal, this is usually a 2% sulphuric acid solution [11]. The membrane contactor itself is a parallel tube system (hollow fiber module), in our case wastewater on the "shell side", while sulphuric acid flows in the hollow fiber [11].

The flow can be turbulent ($\mathrm{Re} > \mathrm{Re_{crit}}$) or laminar ($\mathrm{Re} < \mathrm{Re_{crit}}$), which, through the:

$$\mathrm{Re} = \frac{v \cdot l \cdot \rho}{\eta} \tag{5}$$

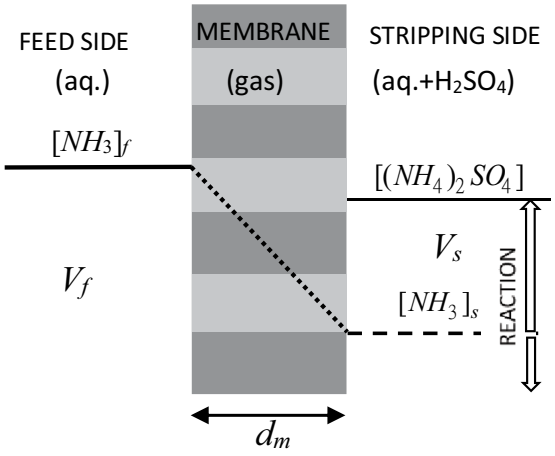

Fig. 1. Scheme of ammonia diffusion through the flat sheet membrane in a single-step model.

Reynolds number, depends on the flow rate [22], where v is the flow rate, η is the viscosity, and l is the characteristic length. From Eq. (5) it follows, that if the flow rate is greater than the one associated with the Re_{crit} number, the flow is turbulent, and if it is smaller, the flow is laminar.

A rate difference occurs along the cross-section during flow, since the flow rate by the wall is v = 0 (Fig. 2), so a laminar flow definitely forms here. If the flow rate in the middle exceeds the flow rate associated with Re_{crit}, the flow becomes turbulent. Approaching the edge, the flow at the above-mentioned rate changes to laminar, that is, a laminar boundary layer forms along the wall, as illustrated in Fig. 3.

The transfer of ammonia through the membrane can be explained by means of a resistance-in-series model, which considers the transport phenomena at the proximities of the membrane. The transfer of ammonia can be described by the following sequence of steps: transfer from the bulk of the feed solution through the boundary layer to the feed-membrane interface, diffusion through the membrane pores filled with gas to the receiving solution interface, the reaction on the interface, and diffusion of the ammonium salt into the extraction solution.

In a parallel study [12] – consistent with other authors [18–20] – a chemical reaction was demonstrated, and therefore the subsequent process does not have a significant effect on the value of the (total) mass transfer coefficient K, so it is sufficient to consider the first two processes, the transfers through the feed-side boundary layer and through the membrane (double-step model) as it can be seen in Fig. 3.

2.5. Membrane mass transfer coefficient

The flux through the membrane analogously with Eq. (1) and according to Fig. 3 is as follows:

$$J_m = \frac{\tilde{D}_m}{d_m} \cdot \left[\mathrm{NH_3}\right]_{f,g}^{(i)} \tag{6}$$

where $[NH_3]_{f,g}^{(i)}$ ($[NH_3]_{s,g}^{(i)} = [NH_3]_s = 0$) is the ammonia concentration in the membrane (gaseous) at the feed-membrane interface and d_m is the real thickness of the membrane. $\tilde{D}_m$ the effective diffusion coefficient in the membrane can be estimated from the following equation [14,15]:

$$\tilde{D}_m = \frac{\varepsilon}{\tau} D_m \tag{7}$$

where ε, and τ are the porosity and the tortuosity of the membrane, respectively, furthermore

$$D_m = \frac{\delta}{3}\sqrt{\frac{8R_gT}{\pi M}} \tag{8}$$

can be chosen between a molecular self-diffusion (δ = λ) or the Knudsen diffusion (δ = d_p) depending on the value of the Knudsen number (Kn = λ/d_p) [15], where λ is the molecular mean free path length [23], d_p is the pore diameter (m), and M is the molecular weight (of the ammonia). With membranes in use, the two kinds of diffusion usually occur at the same time [10].

The correlation between the dissolved free ammonia concentration on the feed side, $[NH_3]_f^{(i)}$ and the concentration of free gaseous ammonia in the membrane, $[NH_3]_{f,g}^{(i)}$ is expressed by the Henry constant, H (in water), namely [24]:

$$\frac{\left[\mathrm{NH_3}\right]_{f,g}^{(i)}}{\left[\mathrm{NH_3}\right]_f^{(i)}} = \frac{H}{R_gT} \tag{9}$$

By comparing the molar flux Eq. (6) passing through the membrane and Eq. (9) as the feed-side (dissolved) ammonia concentration, we obtain the following function:

$$J_m = \frac{H}{R_gT}\frac{\tilde{D}_m}{d_m} \cdot \left[\mathrm{NH_3}\right]_f^{(i)} \tag{10}$$

The Henry constant (in water) can also be presented as the function of the temperature [10]:

$$H = H_0 e^{-\frac{E_H}{R_gT}} \tag{11}$$

with E_H = 34 kJ mol^{-1} (in water) and H_0 parameters [24].

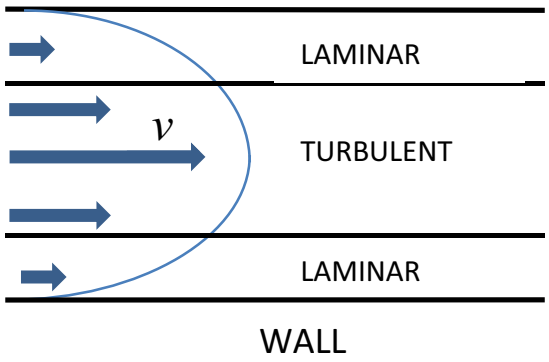

Fig. 2. The liquid flow between two walls. The parabolic is the laminar rate profile.

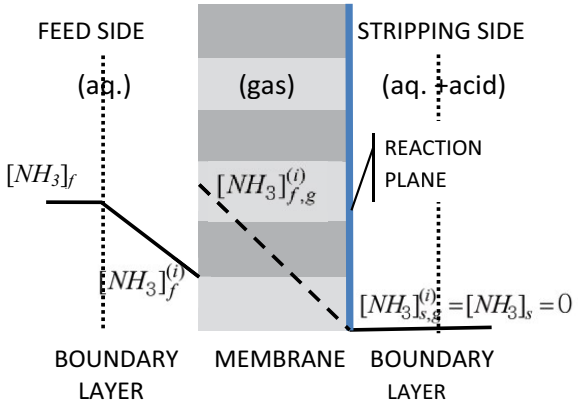

Fig. 3. Scheme of ammonia diffusion through the flat sheet membrane in a double-step model with the laminar boundary layers.

Table 1
Estimated values of the mass transfer coefficient ($\hat{K}$), the mass transfer coefficient (K), the standard errors (s_K) and the confidence intervals at a 95% probability level from [12]

i	Temperature (°C)	$\hat{K}$ (mh^{-1})	s_K (mh^{-1})	K (95%) (mh^{-1})
1	25	0.0105	0.003	0.0097–0.0113
2	32	0.0135	0.003	0.0127–0.0143
3	40	0.0173	0.002	0.0168–0.0178

2.6. Liquid mass transfer coefficient, resistance in series model

Due to the laminar flow, mass transport takes place by diffusion through the feed-side liquid layer. The mass flux passing through, analogously to Eq. (1), will be proportional to the dissolved ammonia concentration difference (Fig. 3), that is:

$$J_f = K_f\left(\left[\mathrm{NH_3}\right]_f - \left[\mathrm{NH_3}\right]_f^{(i)}\right) \tag{12}$$

where K_f is the mass transfer coefficient through the feed-side boundary layer.

The liquid mass transfer coefficient for the species in the shell side, under laminar flow conditions, can be calculated from the Sherwood correlation [15]:

$$\mathrm{Sh} = \frac{K_f \cdot l}{D_w} \tag{13}$$

where D_w is the diffusion constant (of ammonia) in water, and l is the characteristic size (m), which is dependent on the membrane type; in the case of a flat sheet membrane it is the size of the membrane facing the flow, and for a tube membrane the characteristic tube diameter.

For the diffusion coefficient in liquids (water), the Einstein-Stokes correlation is used [25]. For spherical particles, this will be the following:

$$D_w = \frac{R_g T}{6\pi N \eta r} \tag{14}$$

where r is the particle (ammonia molecule) radius, η is the viscosity (in water) of the feed side wastewater, and N is the Avogadro number.

Viscosity as the function of temperature (Fig. 4) can be written as an Arrhenius-type correlation as well:

$$\eta = \eta_0 e^{\frac{E_\eta}{R_g T}} \tag{15}$$

where E_η = 16 kJ mol^{-1} activation energy in water [26].

The diffusion coefficient in liquid by comparing Eqs. (14) and (15)

$$D_w = D_{w,0} e^{-\frac{E_\eta}{R_g T}} \tag{16}$$

also exhibits an Arrhenius-type temperature dependence with the activation energy E_η and the pre-exponential coefficient $D_{w,0} = \frac{R_g T}{6\pi N \eta_0 r}$.

The Sherwood correlation for the species in the shell side of the hollow fibre modules [15]:

$$\mathrm{Sh} = 5.8\left[d_h \frac{1-\Phi}{l}\right] \cdot \mathrm{Re}^{0.6} \cdot \mathrm{Sc}^{0.33} \tag{17}$$

is the function of the Reynolds $\mathrm{Re} = \frac{d_h \nu \rho}{\eta}$ and the Smith $\mathrm{Sc} = \frac{\eta}{\rho \cdot D_w}$ numbers, where d_h and ρ are the dynamic diameters and density of the solution, furthermore Φ and l are the dynamic diameters, packing density and length of the fibers.

Incorporating these values into equation Eq. (17), the Sherwood number is:

$$\mathrm{Sh} = \mathrm{Sh}_0 e^{\frac{0.06 E_\eta}{R_g T}} \tag{18}$$

where $\mathrm{Sh}_0 = 5.8\left[d_h \frac{1-\Phi}{l}\right] a_{\mathrm{Re}}^{0.6} \cdot a_{\mathrm{Sc}}^{0.33}$, furthermore $a_{\mathrm{Re}} = \frac{d_h \nu \rho}{\eta_0}$ and $a_{\mathrm{Sc}} = \frac{\eta_0}{\rho \cdot D_{w,0}}$ are pre-exponential coefficients.

Finally, using Eqs. (13) and (15)–(17) from Eq. (18) the mass transfer coefficient for the transfer through the feed-side boundary layer is the following Arrhenius-type correlation:

$$K_f = K_{f,0} e^{-\frac{0.94 E_\eta}{R_g T}} \tag{19}$$

where $0.94E_\eta$ = 15 kJ mol^{-1} is the activation energy of the process, with the pre-exponential coefficient $K_{f,0} = \frac{\mathrm{Sh}_0 D_{w,0}}{l}$.

2.7. Stripping process

The mass transfer process is followed by a stripping (chemical) process. In the other paper [12] we demonstrated that since the rate constant of the stripping process is considerably higher than that of the transport process, the stripping-side ammonia concentration.

$$\left[\mathrm{NH_3}\right]_s = \left[\mathrm{NH_3}\right]_s^{(i)} \cong 0 \tag{20}$$

is zero with a good approximation, provided the concentration of the stripping-side solvent fluid (sulphuric acid) exceeds a certain value (0.2 mol L^{-1}) [10].

2.8. Total mass transfer coefficient

To determine the full mass transfer coefficient, the feed-side ammonia concentration according to Fig. 3 can be rewritten as $[\mathrm{NH_3}]_f = [\mathrm{NH_3}]_f - [\mathrm{NH_3}]_f^{(i)} + [\mathrm{NH_3}]_f^{(i)}$ with due

consideration of Eq. (20). In a quasi-steady state, $J = J_f = J_m$, therefore dividing before ones by the appropriate flux values that is:

$$\frac{\left[NH_3\right]_f}{J} = \frac{\left[NH_3\right]_f - \left[NH_3\right]_f^{(i)}}{J_f} + \frac{\left[NH_3\right]_f^{(i)}}{J_m} \tag{21}$$

Using equations Eqs. (2) and (10) (considering Eq. (3)) and Eq. (12) the next equation can be written for the total mass transfer coefficient:

$$\frac{1}{K} = \frac{1}{K_f} + \frac{R_g T}{H}\frac{1}{K_m} \tag{22}$$

Substituting Eqs. (4), (11) and (19) into Eq. (22), the following correlation can be achieved for the total mass transfer coefficient, as a function of the temperature in the case of a series model:

$$\frac{1}{K} = \frac{1}{K_0}e^{\frac{E_a}{R_g T}} = \frac{1}{K_{f,0}}e^{\frac{0.94E_\eta}{R_g T}} + \frac{R_g T}{H_0 K_m}e^{\frac{E_H}{R_g T}} \tag{23}$$

2.9. Ratio of sub-processes

Introducing the next proportional number for the pre-exponential coefficients:

$$x_f = \frac{K_0}{K_{f,0}} \quad \text{and} \quad x_m = \frac{R_g T}{H_0}\frac{K_0}{K_m} \tag{24}$$

Eq. (23) can be written in the next form:

$$x_f e^{\frac{0.94E_\eta - E_a}{R_g T}} + x_m e^{\frac{E_H - E_a}{R_g T}} = 1 \tag{25}$$

Let us take two extreme temperatures of the measurement range, T_{min} and T_{max}. Since E_a, activation energy values can be determined from the measured values, while E_η and E_H are also known, using these, we can calculate x_f and x_m as the solutions of an equation system with two variables. Knowing the above values, the direction of the two sub-processes can be determined within the full process, which is:

$$\mathbf{R}_f = e^{\frac{0.94E_\eta - E_a}{R_g T}} \quad \text{and} \quad \mathbf{R}_m = x_m e^{\frac{E_H - E_a}{R_g T}} \tag{26}$$

since $\mathbf{R}_f + \mathbf{R}_m = 1$, therefore $\mathbf{R}_f$:$\mathbf{R}_m$ means the ratio of two sub-processes within the total mass transfer process.

3. Results

3.1. Mass transfer coefficient

To validate the model, the estimated values ($\hat{K}$) of the mass transfer coefficient (K) with the standard errors (s_K) and confidence intervals at a 95% probability level have been used from one of our parallel studies [12]. The data are in Table 1, where K (95%) is the confidence interval at a 95% probability level where the mass transfer coefficient, K stays with a probability of 95% in. Further details connected to the measurement and the result are found in an earlier [11] and parallel [12] work.

3.2. Estimation of activation energy

The value of activation energy has been estimated by linear regression [12]. Taking the logarithm of Eq. (4) the regression line will be:

$$y = ax + b \tag{27}$$

where $y = \ln \hat{K}$, $a = -E_a$, $x = -\frac{1}{R_g T}$ and $b = \ln K_0$ (Fig. 4), from this $\hat{E}_a$ = 26.2 kJ mol^{-1}. Furthermore, R^2 and t_{n-2} have been calculated, where $f = n-2$ is the variability and n the number of the elements (measured data) [12], n = 3, p = 2 and R^2 = 0.9988, based on which t_f = 28.9 and $t_{1,0.95}$ = 6.31 (student-test table). The 0-hypothesis H_0:$\hat{E}_a = E_a$ has been accepted at a 95% probability level as $t_{n-2} > t_{1,0.95}$.

3.3. Standard error of estimation, confidence interval

The standard errors of parameters, s_a and s_b were calculated by the known formulas referred to in parallel work in this volume [12]. Finally, a confidence interval (both sides) of 95% has been determined for a will be $[\hat{a} - t_{f,0.975}s_a; \hat{a} + {}_{f,0.975}s_a]$ and for b as well. P = 1–0.95 = 0.05 is the significance level (interval estimation) [12]. Now n = 3 and the standard error of activation energy is s_E = 0.29 kJ mol^{-1}. The confidence interval (both sides) of 95% is $[\hat{E}_a - t_{1,0.975}s_E; \hat{E}_a - t_{1,0.975}s_E]$, that is [22.7–29.7 kJ mol^{-1}], and P = 1–0.95 = 0.05 is the significance level – [12] – meaning the probability that E_a is outside the confidence interval in the case of a 0-hypothesis.

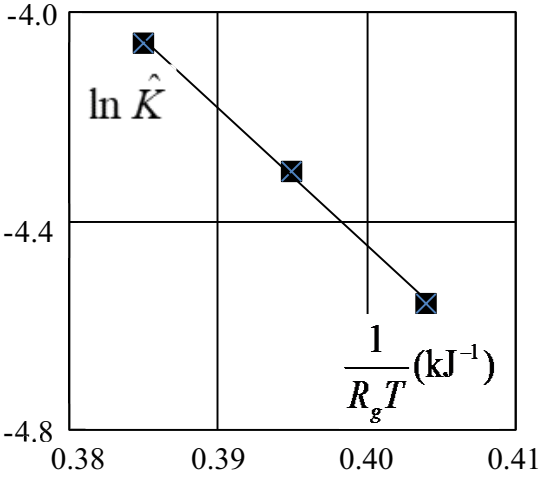

Fig. 4. The logarithm of estimated mass transfer coefficient, $\hat{K}$ as a function of reverse temperature, T for determination of activation energy, E_a.

4. Discussion

The activation energy of the mass transfer coefficient, E_a = 26.2 kJ mol^{-1} [22.7–29.7 kJ mol^{-1}], is a good approximation for values acquired in similar studies [9–10] in similar ranges, 26 and 31 kJ mol^{-1} respectively. These and my values are higher than the 0–15 kJ mol^{-1} activation energy that can generally be achieved for diffusion processes [27,28].

Assuming full equalization for both the feed and receiving side, the total mass transfer coefficient K consists of two parts (double-step model). One belongs to the mass transfer on the feed side, on the boundary layer that forms during the flow K_f. The calculated value of the activation energy associated with this is $0.94 \times E_\eta \cong 15$ kJ mol^{-1}, which is somewhat smaller than that of the diffusion in liquid E_η = 16 kJ mol^{-1} derived from the temperature dependence of viscosity. The reason for the difference is that the energy dependence of the flow's Sherwood number decreases the activation energy of the mass transfer coefficient K_f.

Since the mass transfer coefficient of the transmembrane process is only marginally dependent on temperature (please note that this can also be expressed in the Arrhenius form with an activation energy of approximately 0), the activation energy for the whole process must be less than 15 kJ. It is greater because of the temperature dependence of the Henry number. The associated activation energy determines that of the transmembrane process, not through the mass transfer coefficient but the concentration gradient. In this case, the activation energy comes from the feed-side boundary transfer of the membrane and would be the consequence of the Arrhenius-type temperature dependence of the Henry constant. As a result, the activation energy E_a of the whole mass transfer process can be between the two mentioned values (15–34 kJ mol^{-1}) depending on the $\mathbf{R}_f$:$\mathbf{R}_m$ ratio of the two processes vis-a-vis each other.

Knowing the calculated activation energies for the two sub-processes and the measured activation energies for the total process, based on Eqs. (24)–(26), the ratio of the two sub-processes can be determined. According to my own data and data from the literature, the activation energy for the full process can be 25–30 kJ mol^{-1}. Using this, for a flat sheet membrane at 25°C, $\mathbf{R}_f$:$\mathbf{R}_m$ = (0.7–0.9):(0.3–0.1) at 40°C $\mathbf{R}_f$:$\mathbf{R}_m$ = (0.5–0.7):(0.5–0.3), for tube membrane at 25°C $\mathbf{R}_f$:$\mathbf{R}_m$ = (0.8–0.95):(0.2–0.05) at 40°C $\mathbf{R}_f$:$\mathbf{R}_m$ = (0.6–0.8):(0.4–0.2), that is, the larger part in the measurement range pertains to the transfer through the membrane.

The mass transfer coefficient for the membrane K_m is a function of the characteristics (porosity, thickness, tortuosity) of the membrane material, while K_f on the feed-side boundary layer is the function of the flow characteristics (a type of flow, membrane type, and parameters). All these factors together determine the value of the total mass transfer coefficient.

The activation energy of the whole process, E_a, means the energy that could be measured in the case of a single-process model. Accordingly, this is a virtual value and cannot be linked to any physical phenomenon, only the two sub-processes have it. Thus both K_f [11,12] and E_a [9,10] can be dependent on the measuring conditions and apparatus used.

5. Conclusion

The mass transfer coefficient exhibits an Arrhenius-type temperature dependence. By increasing the temperature, the value of the mass transfer coefficient, that is the rate of the process, can also be increased, so the necessary treatment time can be decreased. However, it must also be considered that there are limits for increasing the temperature, primarily concerning the useful life of the membrane. By measuring the temperature, the model can be used to optimize treatment time. The mass transfer coefficient can also be increased by optimizing the membrane contactor material, and specifically the membrane material. Nevertheless, its limitations, primarily on selectivity, must be considered in this case.

Acknowledgements

3 M and Liqui-Cel are trademarks of 3 M Company. The project was supported by GINOP-2.3.2-15-2016-00016 Excellence of Strategic R+D workshops entitled "Development of modular, mobile water treatment systems and wastewater treatment technologies at University of Pannonia to enhance growing, dynamic exports of Hungary (2016–2020)".

Symbols

D	—	Diffusion coefficient, m^2 s^{-1}
E	—	Energy, kJ mol^{-1}
H	—	Henry constant, mol Mpa^{-1}
J	—	Flux, mol m^{-2} h^{-1}
K	—	Mass transfer coefficient, mh^{-1} mmin^{-1}
Kn	—	Knudsen number, –
N	—	Avogadro number, 6.02 × 10^{23} molecules mol^{-1}
P	—	Significance level
R_g	—	Gas constant, kJ mol^{-1} K^{-1}
$\mathbf{R}$	—	Rate, –
Re	—	Reynolds number, –
Sc	—	Smith number, –
Sh	—	Sherwood number, –
T	—	Treatment temperature, K, °C
V	—	Volume, volume liquid/reservoir, m^3
[X]	—	Solute concentration, mol m^{-3}, mg L^{-1}
K_x	—	Pre-exponential coefficient, mh^{-1}, mmin^{-1}
a	—	Parameter
b	—	Parameter
d	—	Diameter, thickness, m
l	—	Diffusion length, m
n	—	Number of samples
r	—	Radius of ammonia molecule, m
t	—	Time, h, min
t_f	—	Student-test
ε	—	Porosity, –
λ	—	Mean free path length, m
τ	—	Tortuosity, –
η	—	Viscosity of water, Pa s

ν — Velocity, ms^{-1}
ρ — Density of water, kg m^{-3}

Indexes

0 — Initial value, pre-exponential
a — Activation
f — Feed side
f — Variability
i — Interface
g — Gas
m — Membrane
s — Stripping side
t — Belonging to *t* time
w — Water
^ — Estimated value

References

[1] M.C.S. Amara, N.C. Magalhães, W.G. Moravia, C.D. Ferreira, Ammonia recovery from landfill leachate using hydrophobic membrane contactors, Water Sci. Technol., 74 (2016) 2177–2184.
[2] E.E.L. Bernal, C. Maya, C. Valderrama, J.L. Cortina, Valorization of ammonia concentrates from treated urban wastewater using liquid–liquid membrane contactors, Chem. Eng. J., 302 (2016) 641–649.
[3] M. Darestani, V. Haigh, S.J. Couperthwaite, G.J. Millar, L.D. Nghiem, Hollow fibre membrane contactors for ammonia recovery: current status and future developments, J. Environ. Chem. Eng., 5 (2017) 1349–1359.
[4] M. Rezakazemi, S. Shirazian, S.N. Ashrafizadeh, Simulation of ammonia removal from industrial wastewater streams by means of a hollow-fiber membrane contactor, Desalination, 285 (2012) 383–392.
[5] M.J. Rothrock Jr., A.A. Szögi, M.B. Vanotti, Recovery of ammonia from poultry litter using flat gas permeable membranes, Waste Manage., 33 (2013) 1531–1538.
[6] I. Sancho, E. Licon, C. Valderrama, N. de Arespacochaga, S. López-Palau, J.L. Cortina, Recovery of ammonia from domestic wastewater effluents as liquid fertilizers by integration of natural zeolites and hollow fibre membrane contactors, Sci. Total Environ., 584–585 (2017) 244–251.
[7] X.Y. Tan, S.P. Tan, W.K. Teo, K. Li, Polyvinylidene fluoride (PVDF) hollow fibre membranes for ammonia removal from water, J. Membr. Sci., 271 (2006) 59–68.
[8] M.B. Vanotti, P.J. Dube, A.A. Szogi, M.C. García-González, Recovery of ammonia and phosphate minerals from swine wastewater using gas-permeable membranes, Water Res., 112 (2017) 137–146.
[9] J. Preez, B. Norddahl, K. Christensen, The BIOREK® concept: a hybrid membrane bioreactor concept for very strong wastewater, Desalination, 183 (2005) 407–415.
[10] A. Hasanoğlu, J. Romero, B. Pérez, A. Plaza, Ammonia removal from wastewater streams through membrane contactors: experimental and theoretical analysis of operation parameters and configuration, Chem. Eng. J., 160 (2010) 530–537.
[11] M. Ulbricht, G. Lakner, J. Lakner, K. Bélafi-Bakó, Trans-MembraneChemiSorption of ammonia from sealing water in Hungarian powder metallurgy furnace, Desal. Water Treat., 75 (2017) 253–259.
[12] G. Lakner, J. Lakner, P. Bakonyi, K. Bélafi-Bakó, Kinetics of TransMembraneChemiSorption for waste water with high ammonia contents, Desal. Water Treat., (2020), doi: 10.5004/dwt.2020.25872.
[13] Z.Z. Zhu, Z.L. Hao, Z.S. Shen, J. Chen, Modified modeling of the effect of pH and viscosity on the mass transfer in hydrophobic hollow fiber membrane contactors, J. Membr. Sci., 250 (2005) 269–275.
[14] H. Mahmud, A. Kumar, R.M. Narbaitz, T. Matsuura, A study of mass transfer in the membrane air-stripping process using microporous polyproplylene hollow fibers, J. Membr. Sci. 179 (2000) 29–41.
[15] Gabelman, S. Hwang, Hollow fiber membrane contactors, J. Membr. Sci., 159 (1999) 61–106.
[16] M.H.V. Mulder, Basic Principles of Membrane Technology, Kluwer Academic Publishers, Dordrecht, 1996.
[17] H. Kreulen, C.A. Smolders, G.F. Versteeg, W.P.M. van Swaaij, Microporous hollow fibre membrane modules as gas-liquid contactors. Part 1. Physical mass transfer processes: a specific application: mass transfer in highly viscous liquids, J. Membr. Sci., 78 (1993) 197–216.
[18] Z. Qi, E.L. Cussler, Hollow fiber gas membranes, AIChe J., 31 (1985) 1548–1553.
[19] M.J. Semmens, D.M. Foster, E.L. Cussler, Ammonia removal from water using microporous hollow fibers, J. Membr. Sci., 51 (1990) 127–140.
[20] A. Sengupta, A. Pitmann, Application of Membrane Contactors as Mass Transfer Devices, A.K. Pabby, Ed., Handbook of Membrane Separations: Chemical, Pharmaceutical and Biotechnological Applications, CRC Press, Taylor and Francis Group, Boca Raton, 2009, pp. 7–24.
[21] T. Erdey-Grúz, Fundamentals of Physical-Chemistry, Műszaki Kiadó, Budapest, 1972, pp. 467–476.
[22] O. Reynolds, An experimental investigation of the circumstances which determine whether the motion of water shall be direct or sinuous, and of the law of resistance in parallel channels, Philos. Trans. R. Soc. London, Ser. A, 174 (1883) 935–982.
[23] D. Green, R. Perry, Perry's Chemical Engineer's Handbook, 4th ed., McGraw Hill, New York, 2004.
[24] R. Sander, Compilation of Henry's law constants (version 4.0) for water as solvent, Atmos. Chem. Phys., 15 (2015) 4399–4981.
[25] M.V. Reeks, O. Simonin P. Fede, PDF Models for Particle Transport Mixing and Collisions in Turbulent Flow, E.E. Michaelides, C.T. Crowe, J.D. Schwarzkopf, Eds., Multiphase Flow Handbook, CRC Press, Boca Raton, London, New York, 2016.
[26] Water – Dynamic and Kinematic Viscosity, The Engineering Toolbox, 2020. Available at: https://www.engineeringtoolbox.com/water-dynamic-kinematic-viscosity-d_596.html
[27] T.P. Labuza, Shelf-life dating of foods, Food & Nutrition Press, Inc., Westport, Connecticut, USA, 1982, pp. 57–62.
[28] S. Yan, C. Huawei, Z. Limin, R. Fazheng, Z. Luda, Z. Hengtao, Development and characterization of a new amylase type time–temperature indicator, Food Control, 19 (2008) 315–319.